The remarkable influence of $M_2\delta$ to thienyl π conjugation in oligothiophenes incorporating MM quadruple bonds

G. T. Burdzinski[†], M. H. Chisholm[†‡], P.-T. Chou[§], Y.-H. Chou[†], F. Feil[†], J. C. Gallucci[†], Y. Ghosh[†], T. L. Gustafson[†], M.-L. Ho[§], Y. Liu[†], R. Ramnauth[†], and C. Turro[†]

[†]Department of Chemistry, Ohio State University, 100 West 18th Avenue, Columbus, OH 43210-1185; and [§]Department of Chemistry, National Taiwan University, No. 1, Section 4, Roosevelt Road, Taipei 10617, Taiwan

Contributed by M. H. Chisholm, August 14, 2008 (sent for review May 1, 2008)

Oligothiophenes incorporating MM quadruple bonds have been prepared from the reactions between $Mo_2(TiPB)_4$ (TiPB = 2,4,6-triisopropyl benzoate) and 3′,4′-dihexyl-2,2′-:5′,2″-terthiophene-5,5″-dicarboxylic acid. The oligomers of empirical formula $Mo_2(TiPB)_2(O_2C(Th)\text{-}C_4(n\text{-hexyl})_2S\text{-}(Th)CO_2)$ are soluble in THF and form thin films with spin-coating (Th = thiophene). The reactions between $Mo_2(TiPB)_4$ and 2-thienylcarboxylic acid (Th-H), 2,2′-bithiophene-5-carboxylic acid (BTh-H), and (2,2′:5′,2″-terthiophene)-5-carboxylic acid (TTh-H) yield compounds of formula *trans*-$Mo_2(TiPB)_2L_2$, where L = Th, BTh, and TTh (the corresponding thienylcarboxylate), and these compounds are considered as models for the aforementioned oligomers. In all cases, the thienyl groups are substituted or coupled at the 2,5 positions. Based on the x-ray analysis, the molecular structure of *trans*-$Mo_2(TiPB)_2(BTh)_2$ reveals an extended Lπ-$M_2\delta$-Lπ conjugation. Calculations of the electronic structures on model compounds, in which the TiPB are substituted by formate ligands, reveal that the HOMO is mainly attributed to the $M_2\delta$ orbital, which is stabilized by back-bonding to one of the thienylcarboxylate π^* combinations, and the LUMO is an in-phase combination of the thienylcarboxylate π^* orbitals. The compounds and the oligomers are intensely colored due to $M_2\delta$–thienyl carboxylate π^* charge transfer transitions that fall in the visible region of the spectrum. For the molybdenum complexes and their oligomers, the photophysical properties have been studied by steady-state absorption spectroscopy and emission spectroscopy, together with time-resolved emission and transient absorption for the determination of relaxation dynamics. Remarkably, THF solutions the molybdenum complexes show room-temperature dual emission, fluorescence and phosphorescence, originating mainly from ^{1}MLCT and ^{3}MM($\delta\delta^*$) states, respectively. With increasing number of thienyl rings from 1 to 3, the observed lifetimes of the ^{1}MLCT state increase from 4 to 12 ps, while the phosphorescence lifetimes are ≈80 μs. The oligomers show similar photophysical properties as the corresponding monomers in THF but have notably longer-lived triplet states, ≈200 μs in thin films. These results, when compared with metallated oligothiophenes of the later transition elements, reveal that $M_2\delta$–thienyl π conjugation leads to a very small energy gap between the ^{1}MLCT and ^{3}MLCT states of <0.6 eV.

photophysics | dual emission

Because of their potential applications in optoelectronic and magnetic devices, conjugated organic polymers have received much attention (1–3), and oligothiophenes, which constitute one important subclass of these materials, have been found to show excellent hole transport properties (3–7). We have been interested for some time in incorporating MM quadruple bonds into these oligomers by use of the carboxylate tether (8–10), such that the $M_2\delta$ electrons can be brought into conjugation with an extended π-framework of the thiophene moiety. As shown in Scheme 1, the out-of-phase combination of the carboxylate π^* orbitals mix strongly with the $M_2\delta$ orbital whereas the in-phase combination has no symmetry match (11).

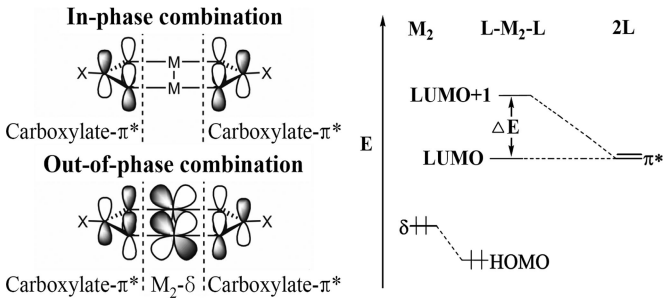

Scheme 1. Mixing of *trans*-L π^* combinations with the M_2 δ.

Earlier studies in this laboratory have drawn a conclusion that the orbital energy of the $M_2\delta$ lies between the filled thienyl valence π-band and its empty π^* band (8, 10). Moreover, the $M_2\delta$ orbital energy can be tuned by selection of the metal, e.g., Mo vs. W, as well as the attendant ligands at the dinuclear center (8). In this article, we report our studies of the photophysical properties of oligothiophenes incorporating MM quadruple bonds with attendant 2,4,6-triisopropylbenzoate ligands, TiPB. By virtue of steric bulk and alkylation, we achieved *trans*-substitution at the dinuclear center and enhanced solubility. The dicarboxylate linker used in the oligomer syntheses is depicted in Scheme 2 *Upper*. To maximize π-conjugation along the thienyl chain, we have maintained the 2,5-substitution pattern at the core C_4S ring, while *n*-hexyl substituents are introduced at C(3) and C(4) position to increase solubility (5, 12–20).

The oligomers derived from the dicarboxylate linkers are also compared with the discrete molecular complexes of the type *trans*-$M_2(TiPB)_2L_2$ (L = thienyl carboxylates) shown in Scheme 2 *Lower*.

A preliminary communication on some relevant aspects of this work was published (11) wherein we noted that the thin films of the oligomers showed electroluminescence when fabricated into an LED device (21, 22). We also note that other groups, in particular Wolf and Raithby and their respective coworkers (23–27), have incorporated certain metal ions into oligothiophenes, but their focus was mostly on elements of the later transition metals.

Author contributions: M.H.C. designed research; G.T.B., Y.-H.C., F.F., Y.G., M.-L.H., Y.L., and R.R. performed research; J.C.G. contributed new reagents/analytic tools; P.-T.C., T.L.G., and C.T. analyzed data; and M.H.C., P.-T.C., Y.-H.C., Y.G., T.L.G., Y.L., and C.T. wrote the paper.

The authors declare no conflict of interest.

Data deposition: The atomic coordinates have been deposited in Cambridge Structural Data Centre (CCDC).

‡To whom correspondence should be addressed. E-mail: chisholm@chemistry.ohio-state.edu.

This article contains supporting information online at www.pnas.org/cgi/content/full/0807411105/DCSupplemental.

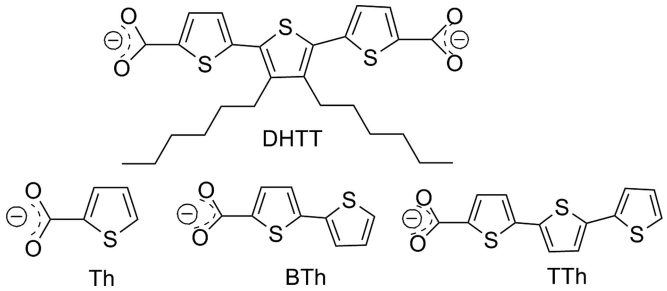

Scheme 2. Structures of the ligands.

Results and Discussion

Structure of $Mo_2(TiPB)_2(BTh)_2$. To provide some structural insight into the nature of the species under consideration, we undertook a single-crystal x-ray structural determination of the compound $Mo_2(TiPB)_2(BTh)_2$. An ORTEP drawing of the molecular structure is shown in Fig. 1.

In the solid state, there are pairs of Mo_2 units that are related by a crystallographically imposed inversion center. The Mo_2 units are linked via the agency of weak Mo···carboxylate oxygen bonds, as is often seen in the laddered structures of $Mo_2(O_2CR)_4$ compounds (8). The Mo_2 unit is also ligated by a weakly bound THF molecule. This long Mo···O bond distance is 2.554(4) Å. Full structural details are given in supporting information (SI) Tables S1–S5.

The *trans*-substitution at the dinuclear unit is anticipated based on steric considerations and was previously observed in a related bisazulenecarboxylate compound supported by two TiPB ligands and in $Mo_2(TiPB)_2(Th)_2$ (10). The orientation of the aryl ring of one of the TiPB ligands is twisted by an angle of 73.9° from the plane containing Mo-Mo and the associated carboxylate group to minimize steric repulsive interactions, resulting in the loss of conjugation between the π-orbitals of the phenyl ring and the $M_2\delta$ orbital. The analogous dihedral angle for the other TiPB ligand is 77.4°. In contrast, the *trans*-BTh ligands are nearly planar and hence maximize the $L\pi$–$M_2\delta$–$L\pi$ conjugation. It is reasonable to anticipate that a similar structure is adopted for the terthienyl carboxylate compound of formula $Mo_2(TiPB)_2(TTh)_2$ and also for the *trans*-substituted oligomers. Evidence for this type of extended π-conjugation is seen in the UV-visible absorption spectra, which reveal a bathochromic shift of the ^{1}MLCT transition with increasing number of thienyl rings (*vide infra*). It should be noted that in low viscous solvents such as THF the rotational barrier of the C–C bonds for both carboxylate–thienyl and thienyl–thienyl rings is expected to be low, compared with thermal energy. For the oligomers, the introduction of the 3,4-hexyl substituents will impede the ground-state planarity due to steric hindrance, and this leads to a broadening of the ^{1}MLCT absorptions (*vide infra*).

Electronic Structure Calculations. To gain insight into the correlation between electronic structures and spectroscopic properties (UV-visible absorption and emission) of the species under consideration, we carried out electronic structure calculations on the model compounds *trans*-$Mo_2(HCO_2)_2L_2$, where L = Th, BTh, and TTh, by employing density functional theory (DFT) (28–31) as implemented in the Gaussian 03 programs (32). Geometry optimization was performed under C_i and C_1 symmetry, and details are elaborated on in *SI Materials and Methods*. In brief, the HOMO was calculated to be mainly the $Mo_2\delta$ orbital that is further stabilized via π-back-bonding to the out-of-phase combination of the two thienyl carboxylate π^* orbitals. Such a configuration is consistent with that depicted in Scheme 1. This stabilization of the $M_2\delta$ is, however, offset by the filled π interactions with the thienyl carboxylate ligands as seen in the electrochemical data (*vide infra*).

The nature of the unoccupied lowest-energy orbitals depends on the number of thienyl rings. For one thiophene ring, the LUMO is calculated to be the $Mo_2\delta^*$ orbital, and the LUMO +1 and LUMO +2 are the in-phase and out-of-phase thienyl carboxylate π^* orbitals, respectively, as anticipated from Scheme 1. With two thienyl rings, the $M_2\delta^*$ orbital lies between the in-phase and out-of-phase ligand π^* orbitals, whereas for the terthienyl carboxylate, the $M_2\delta^*$ orbital lies above both. Qualitatively, the energy separation between the in-phase and out-of-phase thienyl carboxylate π^* orbitals is a measure of the degree of $M_2\delta$ to ligand π^*-back-bonding. As the number of thienyl rings increase, the orbital energies of the ligand π^* orbitals fall. Conversely, π-conjugation increases the relative energies of the filled ligand based π orbitals. These frontier orbitals are shown for the three model compounds in Fig. 2.

Time-dependent DFT calculations were also carried out, and these predict that the lowest-energy electronic transitions of high

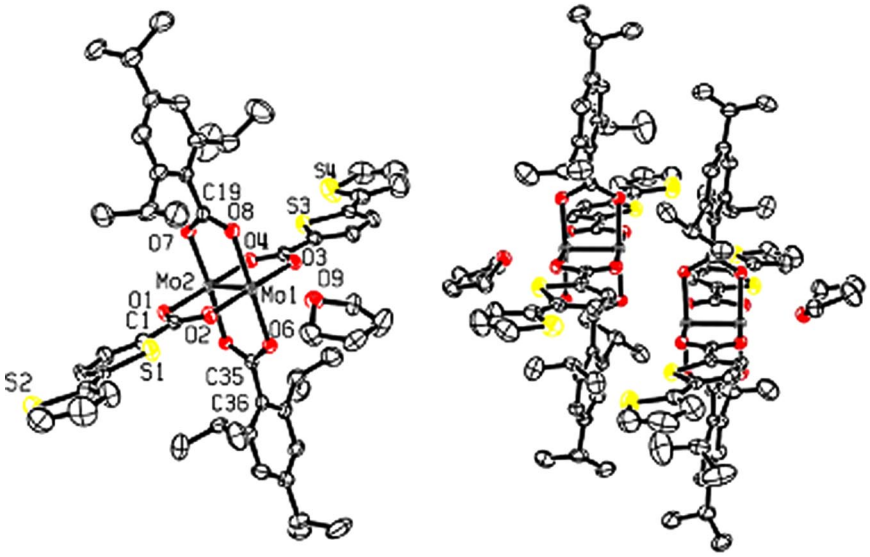

Fig. 1. Crystal structure (*Left*) and packing diagram (*Right*) for $Mo_2(TiPB)_2(BTh)_2$. A disordered solvent molecule of THF is omitted for clarity.

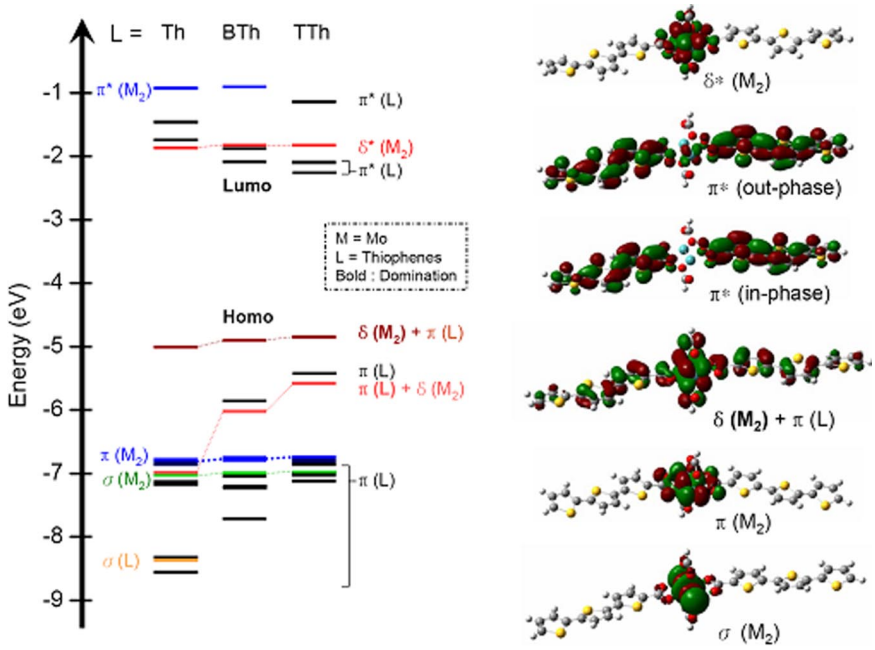

Fig. 2. Energy level diagram of frontier molecular orbitals for $Mo_2(HCO_2)_2L_2$ model compounds, where L = Th, BTh, and TTh. Selected frontier molecular orbital plots calculated for $Mo_2(HCO_2)_2(TTh)_2$. Note that the orbitals are drawn with an isosurface value of 0.02.

intensity correspond to $M_2\delta \rightarrow$ ligand π^* and that these move to lower energy with increasing number of rings, n. The $M_2\delta$-to-δ^* singlet transitions are weak by comparison and are anticipated to be masked by the ^{1}MLCT. At higher energy, the calculations predict intense absorptions due to ligand π-to-π^* transitions, ^{1}LLCT, and with increasing n these also move to lower energy. Qualitatively, the time-dependent DFT predictions are consistent with expectations based on the molecular orbital energy level diagram shown in Fig. 2.

Electrochemical Studies. The compounds $Mo_2(TiPB)_2L_2$ were studied by cyclic voltammetry. In THF solutions, they all show one reversible oxidation wave close to the $Cp_2Fe^{0/+}$ couple. With increasing number of rings, this oxidation becomes easier. The complexes also show quasi-reversible reduction waves, which we associate with thienyl ring reductions. With increasing number of rings, these reduction waves also move to lower potentials, as might be expected from both the electronic structure calculations and also simple considerations of charge delocalization. The differential-pulse voltammogram (DPV) and cyclic voltammogram (CV) curves corresponding to the oxidation of the Mo_2 centers and reduction of the thienyl ring, respectively, are shown in Fig. S1, and the oxidation potentials are listed in Table 1.

Absorption Spectra. A comparison of the room-temperature electronic absorption spectra for the three compounds in THF and the oligomer in THF and as a thin film are shown in Fig. 3. As predicted by the time-dependent DFT calculations, both the ^{1}MLCT and the ^{1}LLCT move to lower energy with increasing number of rings. The similarity between the model compound $Mo_2(TiPB)_2(TTh)_2$ and the oligomer is quite apparent. The broadness—i.e., full width at half maximum (FWHM)—of the ^{1}MLCT arises from the Boltzmann distribution of dihedral angles between the O_2C–ring–ring planes at room temperature. In solution, the oligomer is only slightly broader in its spectral features than the discrete complex $Mo_2(TiPB)_2(TTh)_2$, but as a thin film, it is notably broader. A comparison of the observed and calculated spectral data is given in Table 1.

Emission Spectra. The compounds under consideration show room-temperature dual emission: both fluorescence and phosphorescence. Because of instrumental limitations, a quantitative comparison of fluorescence and phosphorescence was difficult. The singlet and triplet emission spectra are shown in Fig. 4.

At low temperature, emissions assigned to the ^{1}MLCT states show vibronic features associated with the aromatic carboxylate group ($\approx$1,150 cm^{-1}) (see Fig. S2). The emission lifetimes are estimated by up-conversion to be $\approx$20 ps, which supports the view that these are fluorescence.

Excitation spectra confirmed that the fluorescence originated from the compounds and not impurities derived from degradation. The free thienyl carboxylic acids fluoresce with much longer lifetimes, $>$ 100 ps.

The triplet emission is also shown in Fig. 4 for all three

Table 1. Comparison of calculated and experimentally observed properties for the various carboxylate complexes of MM quadruple bonds at 298 K in THF and as a film

	λ_{abs}, nm	λ_{em}, nm	τ (^{1}MLCT), ps	τ (^{3}MM$\delta\delta^*$), μs	λ_{calc}, nm	$E_{1/2}$, V
$Mo_2(TiPB)_2Th_2$	443	574	4	77	441	0.50
$Mo_2(TiPB)_2BTh_2$	500	668	7	83	515	0.48
$Mo_2(TiPB)_2TTh_2$	527	707	12	72	559	0.48
$[Mo_2(TiPB)_2DHTT]_x$	519	730	10	37	—	—
$[Mo_2(TiPB)_2DHTT]_x$ (film)	520	700	—	200	—	—

The oxidation potentials are referenced with respect to the $Cp^*_2Fe^{0/+}$ couple.

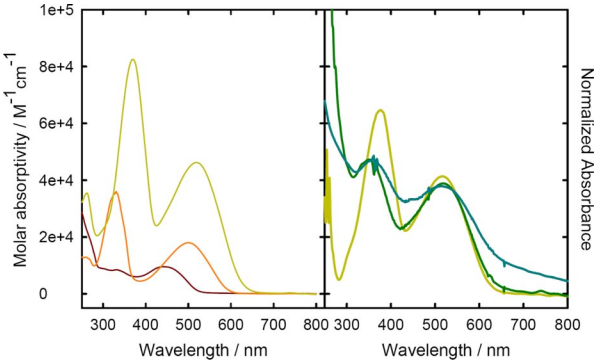

Fig. 3. Absorption spectra of monomer complexes $Mo_2(TiPB)_2L_2$, where L = Th (red), BTh (orange), TTh (dark yellow) (*Left*), and monomer complex $Mo_2(TiPB)_2(TTh)_2$ (dark yellow), oligomer $[Mo_2(TiPB)_2DHTT]_x$ (green) in THF, and $[Mo_2(TiPB)_2DHTT]_x$ thin film (blue) (*Right*).

compounds and the oligomer in THF solution. Quite remarkably, the phosphorescence is virtually identical in all cases. Thus, we see that the energy gap between S_1 and T_1 decreases with increasing number of rings, which is in marked contrast to the findings of Friend and Raithby (33) in their study of metallated conjugated polymers involving platinum. These authors noted that with increasing conjugation the $S_1 \rightarrow S_0$ and $T_1 \rightarrow S_0$ emissions both moved to lower energy and that the S_1–T_1 gap remained relatively constant at ≈0.7 eV.

The emission spectrum of the oligomer in THF is red-shifted with respect to the $Mo_2(TiPB)_2L_2$ compound, which is consistent with greater $M_2\delta$–thienyl π conjugation in the oligomer. However, as a thin film, the oligomer is notably blue-shifted, once again providing an indication of a change in ring–ring and ring–carboxylate dihedral angles in going from solution to the solid state. In the solid state, the extent of $M_2\delta$–ligand π conjugation is reduced.

The estimated lifetimes by emission decay of the phosphorescence ranged from 50 μs for the oligomer to 100 μs for the $Mo_2(TiPB)_2L_2$ compounds in the THF at room temperature (see Fig. S6).

Calculation of the T_1 States and Solvent-Dependent Studies. Puzzled by these findings, we again turned to electronic structure calculations, which predicted that for all three of the model compounds $Mo_2(O_2CH)_2L_2$ where L = Th, BTh, and TTh, the T_1 state was the $^3MM\delta\delta^*$ as shown pictorially by the GaussView plots in Fig. 5. The calculated MM distances for the T_1 state of the molecules were 2.18 Å, which is notably longer than those of the ground state, 2.11 Å.

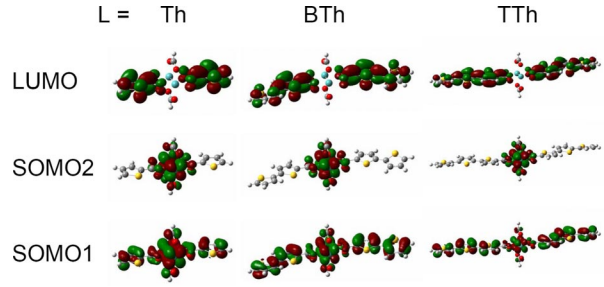

Fig. 5. GaussView plots of the frontier orbitals of the T_1 state of $Mo_2(HCO_2)_2L_2$, where L = Th, BTh, and TTh.

Prompted by these predictions, we examined the absorption and emission spectra of the compound $Mo_2(TiPB)_2(BTh)_2$ in the solvents THF, CH_2Cl_2, Et_2O, MeCN, and MeOH (see Fig. S3). The ^{1}MLCT absorption and emission showed the expected solvatochromism, but the triplet emission did not. This supports the view that the phosphorescence is from the $^3MM\delta\delta^*$ state.

Transient Absorption Spectroscopy. Excitation into the ^{1}LLCT absorption bands gives rise to a transient absorption spectrum that corresponds to that for the ^{1}MLCT state. This indicates that internal conversion (IC) is very rapid and occurs in <300 fs. The transient absorption spectra for the $[Mo_2(TiPB)_2DHTT]_x$ are shown in Fig. 6 with excitation at 347 nm (^{1}LLCT) and 515 nm (^{1}MLCT). The spectra for a similar experiment on $Mo_2(TiPB)_2(TTh)_2$ are shown in Fig. S4. The striking feature in comparing the spectra in these figures is their similarity. Estimates of the lifetimes (shown in Table 1) of the two systems are also within experimental error the same, ≈12 ps. This is a further demonstration of the direct observation of a ^{1}MLCT state for a transition metal complex and complements our earlier report on $Mo_2(O_2C$-9-anthracene$)_4$ (34). We also note that the lifetimes of these transient absorptions are comparable with the lifetimes of

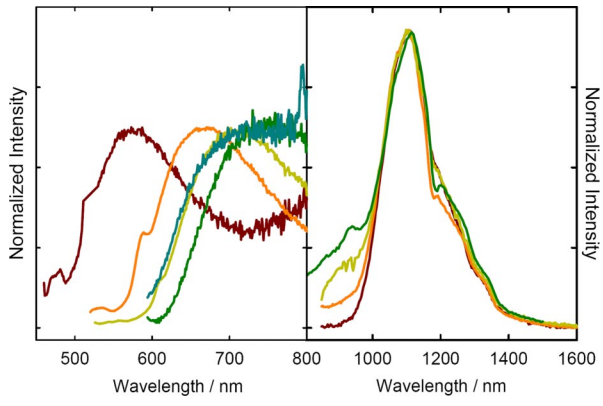

Fig. 4. Photoluminescence spectra of $Mo_2(TiPB)_2L_2$ complexes. (*Left*) Fluorescence spectra of monomer complexes $Mo_2(TiPB)_2L_2$, where L = Th (red), BTh (orange), TTh (dark yellow), and oligomer $[Mo_2(TiPB)_2DHTT]_x$ (green) in THF and $[Mo_2(TiPB)_2DHTT]_x$ thin film (blue). (*Right*) Phosphorescence spectra of monomer complexes $Mo_2(TiPB)_2L_2$, where L = Th (red), BTh (orange), TTh (dark yellow), and oligomer $[Mo_2(TiPB)_2DHTT]_x$ (green) in THF.

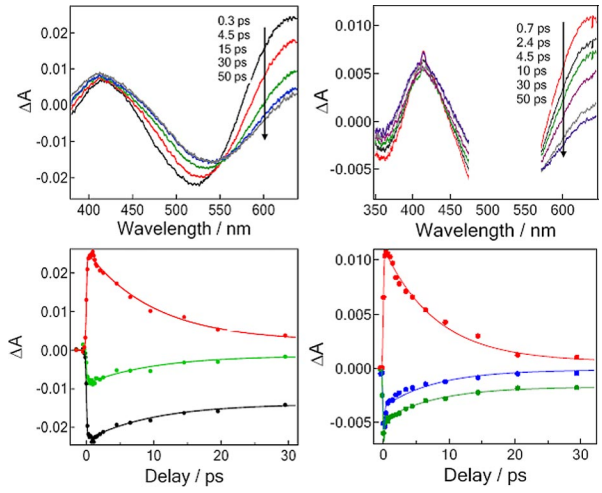

Fig. 6. Femtosecond transient absorption spectra of $[Mo_2(TiPB)_2DHTT]_x$ oligomer in THF excited at 347 nm (*Left*) and 515 nm (*Right*), respectively. The red lines in *Lower* are the time delay spectra collected at 630 nm, whereas the green, black, and blue lines are the time delay spectra collected at 470, 520, and 370 nm, respectively.

the emissions determined by up-conversion. This supports the view that the ultrafast transient absorptions are associated with the emissive states, S_1 (^{1}MLCT).

When the complexes are excited into their ^{1}MLCT states and transient absorption spectra are recorded on the nanosecond time scale, we observed the formation and decay of the T_1 states, now assigned as ^{3}MM$\delta\delta^*$ states. The transient absorption spectra for the three discrete complexes in THF and the oligomer of the terthiophenedicarboxylate, both in THF solution and as a thin film, are shown in Fig. S5. The lifetimes (shown in Table 1) of the ^{3}MM$\delta\delta^*$ states for the discrete complexes $Mo_2(TiPB)_2L_2$ fall in the range of 70–80 μs (see Fig. S6). In contrast, the ^{3}MM$\delta\delta^*$ lifetimes of the oligomers in THF solution are somewhat shorter ($\approx$40 μs) but as a thin film are notably longer ($\approx$200 μs). We attribute the different triplet lifetimes of the oligomers from those of the discrete complexes to the relative rates of triplet–triplet quenching. In solution these are greater for the oligomers as a result of diffusion, whereas as a thin film these are suppressed because of the lack of motion.

The lifetimes of the long-lived transient absorptions support the view that these originate from the phosphorescent states.

A Jablonski diagram summarizing the photophysical properties of the terthienyl complex and its related oligomer is shown in Fig. S7. This again reveals the striking similarities of the two systems with the exception of the lifetimes of the ^{3}MM$\delta\delta^*$ states for the oligomers in solution and as thin films. For the thin films, we were not able to determine the rate of intersystem crossing because of the destruction of the thin films under laser irradiation.

Concluding Remarks. The present work reveals several interesting and surprising features concerning the photophysical properties of these oligothiophenes incorporating MoMo quadruple bonds. (*i*) The spectral features of the model compound $Mo_2(TiPB)_2(TTh)_2$ and the oligomer are extremely similar. (*ii*) In comparison to most second- and third-row transition metal complexes, these systems show relatively slow ^{1}MLCT $\rightarrow$ triplet intersystem crossing. The lifetimes of the ^{1}MLCT states, $\tau_{obs} \sim$ 10 ps, can be contrasted with the Intersystem Crossing $\leq$ 200 fs (35–37). (*iii*) With increasing number of rings, the S_1–T_1 gap decreases in contrast to previous observations of metallated oligothiophenes (33). For the species with three thiophene rings, the S_1–T_1 gap is $\approx$5,000 cm^{-1} or $\approx$0.6 eV. If we accept that the T_1 state is the ^{3}MM$\delta\delta^*$, this result implies that the ^{3}MLCT state is $<$5,000 cm^{-1} from the ^{1}MLCT state. Given that the typical S_1-to-T_1 energy gap for a conjugated oligothiophene is $\approx$1.25 eV (38, 39), and that Friend and Raithby (33) determined an S_1–T_1 gap of $\approx$0.7 eV for their metallated oligothiophenes, the ^{1}MLCT–^{3}MLCT gap is remarkably small in our molybdenum complexes. This indicates a great deal of mixing of the metal δ and organic π systems to affect such a significant spin-orbit coupling in the MLCT states. Furthermore, Wong *et al.* (40), in their studies of donor–acceptor oligothiophenes incorporating Pt, observed only singlet emission in the range 500–700 nm, and they surmised that triplet emission was not observed because of nonradiative decay of the low-energy triplet state. The incorporation of Mo_2 units into oligothiophenes is unique in generating metal based triplet emission. (*iv*) Based on a knowledge of the relative energies of the $Mo_2\delta$ and $W_2\delta$ orbitals, we anticipate that the notably lower energies of the $W_2\delta$-to-thienyl π^* transitions will lead to T_1 states being ^{3}MLCT for related tungsten complexes.

Further studies of these fascinating systems are clearly warranted.

Materials and Methods

Synthesis. The oligomeric material was prepared in dried toluene from the reactions between $Mo_2(TiPB)_4$ and 1 eq of the respective dicarboxylic acid (shown in Scheme 2 *Upper*). The discrete dinuclear compounds were prepared similarly in dried toluene from the reactions between $Mo_2(TiPB)_4$ and 2 eq of the monocarboxylic acids (shown in Scheme 2 *Lower*). Detailed synthetic methodology was elaborated upon in ref. 10. It is worth noting that the lack of the appearance of diastereotopic methyl groups in the ^{1}H NMR spectra for the compounds $Mo_2(TiPB)_2L_2$ is consistent with the expected *trans*-substitution at the dinuclear unit. A similar situation pertains to the oligomers of empirical formula $[Mo_2(TiPB)_2(O_2C(Th)\text{-}C_4(n\text{-hexyl})_2S\text{-}(Th)CO_2)]$ henceforth identified as $[Mo_2(TiPB)_2DHTT]_x$. However, the propensity of these materials to swell and form gels in THF undoubtedly reflects imperfections in polymer structure such as cis- or tri-substitution by the dicarboxylate linker. The latter would lead to cross-linking. According to ^{1}H NMR spectroscopy, there is little evidence of endgroups or tri-substitution. However, by means of MALDI-TOF mass spectrometry, we do find evidence for shorter chains and molecular loops. Given the facile ligand scrambling for $Mo_2(O_2CR)_4$ compounds (41), which can be brought about by adventitious carboxylic acid or carboxylate anions, these oligomers can be viewed to exist as a dynamic equilibrium of species.

Measurements. The measurements of electrochemistry, absorption, emission and nanosecond time-resolved transient absorption were performed according to previously reported procedures (42) and described in detail in *SI Materials and Methods*. Steady-state NIR emission spectroscopy has been reported (43) and is described in detail in *SI Materials and Methods*. The details of femtosecond time-resolved transient absorption and up-conversion experiments are described in *SI Materials and Methods*. The setup of the emission decay was reported in previous works (44).

ACKNOWLEDGMENTS. We thank Professors P. R. Raithby and M. D. Hopkins for their constructive comments, and the Ohio Supercomputer Center for computational resources. We thank the National Science Foundation and the Ohio State Institute for Materials Research for support of the work at Ohio State University, and the National Science Council of Taiwan, Republic of China, for support of work in Taipei.

1. Shirakawa H, Louis EJ, Macdiarmid AG, Chiang CK, Heeger AJ (1977) Synthesis of electrically conducting organic polymers—Halogen derivatives of polyacetylene, (Ch)X. *J Chem Soc Chem Commun*, 578–580.
2. Su WP, Schrieffer JR, Heeger AJ (1979) Solitons in polyacetylene. *Phys Rev Lett* 42:1698–1701.
3. Shirota Y (2000) Organic materials for electronic and optoelectronic devices. *J Mater Chem* 10:1–25.
4. Clot O, Selmarten D, McNevin MJ (2005) Synthesis and characterization of amino-capped oligothiophene-based hole-transport materials. *J Mater Chem* 15:4934–4942.
5. Otsubo T, Aso Y, Takimiya K (2002) Functional oligothiophenes as advanced molecular electronic materials. *J Mater Chem* 12:2565–2575.
6. Kawai K, *et al.* (2005) Synthesis and properties of terthiophene-modified oligodeoxynucleotides. *Bioorg Med Chem Lett* 15:4547–4549.
7. Janzen DE, *et al.* (2004) Preparation and characterization of π-stacking quinodimethane oligothiophenes. Predicting semiconductor behavior and bandwidths from crystal structures and molecular orbital calculations. *J Am Chem Soc* 126:15295–15308.
8. Chisholm MH (2007) Metal to metal multiple bonds in ordered assemblies. *Proc Natl Acad Sci USA* 104:2563–2570.
9. Byrnes MJ, *et al.* (2004) Thienyl carboxylate ligands bound to and bridging MM quadruple bonds, M = Mo or W: Models for polythiophenes incorporating MM quadruple bonds. *Inorg Chem* 43:6334–6344.
10. Chisholm MH, Epstein AJ, Gallucci JC, Feil F, Pirkle W (2005) Oligothiophenes incorporating metal-metal quadruple bonds. *Angew Chem Int Ed* 44:6537–6540.
11. Barybin MV, Chisholm MH, Patmore NJ, Robinson RE, Singh N (2007) Concerning the molecular and electronic structure of a tungsten-tungsten quadruply bonded complex supported by two 6-carboethoxy-2-carboxylatoazulene ligands. *Chem Commun*, 3652–3654.
12. Vidal PL, *et al.* (2000) π-Conjugated ligand polymers entwined around copper centres. *Chem Eur J* 6:1663–1673.
13. Barbarella G, Bongini A, Zambianchi M (1994) Regiochemistry and conformation of poly(3-hexylthiophene) via the synthesis and the spectroscopic characterization of the model configurational triads. *Macromolecules* 27:3039–3045.
14. Matsumoto K, Fujitsuka M, Sato T, Onodera S, Ito O (2000) Photoinduced electron transfer from oligothiophenes/polythiophene to fullerenes (C_{60}/C_{70}) in solution: Comprehensive study by nanosecond laser flash photolysis method. *J Phys Chem B* 104:11632–11638.
15. Lere-Porte JP, Moreau JJE, Torreilles C (1999) Synthesis of regioregular poly(alkylbithiophene)s by an organometallic cross-coupling reaction. *Synth Met* 101:588–589.
16. Donat-Bouillud A, *et al.* (1997) Synthesis, characterization, and processing of new electroactive and photoactive polyesters derived from oligothiophenes. *Chem Mater* 9:2815–2821.
17. Makinoshima T, *et al.* (2004) Competition between intramolecular electron-transfer and energy-transfer processes in photoexcited azulene-C_{60} dyad. *J Phys Chem A* 108:368–375.

18. Janssen RAJ, Moses D, Sariciftci NS (1994) Electron and energy-transfer processes of photoexcited oligothiophenes onto tetracyanoethylene and C_{60}. *J Chem Phys* 101:9519–9527.
19. Kirschbaum T, Briehn CA, Bauerle P (2000) Efficient solid-phase synthesis of regioregular head-to-tail-coupled oligo(3-alkylthiophene)s up to a dodecamer. *J Chem Soc Perkin Trans 1*, 1211–1216.
20. Wang C, *et al.* (1994) Studies on conjugated polymers: Preparation, spectroscopic, and charge-transport properties of a new soluble polythiophene derivative: Poly(3′,4′-dibutyl-2,2′:5′2″-terthiophene). *Chem Mater* 6:401–411.
21. Ho PKH, *et al.* (2000) Molecular-scale interface engineering for polymer light-emitting diodes. *Nature* 404:481–484.
22. Perepichka IF, Perepichka DF, Meng H, Wudl F (2005) Light-emitting polythiophenes. *Adv Mater* 17:2281–2305.
23. Li PY, *et al.* (2002) Metal-metal and ligand-ligand interactions in gold poly-yne systems. *Cryst Eng Commun* 405–412.
24. Khan MS, *et al.* (2003) Synthesis and characterisation of new acetylide-functionalised aromatic and hetero-aromatic ligands and their dinuclear platinum complexes. *Dalton Trans*, 65–73.
25. Zhu YB, Wolf MO (2000) Charge transfer and delocalization in conjugated (ferrocenylethynyl)oligothiophene complexes. *J Am Chem Soc* 122:10121–10125.
26. Stott TL, Wolf MO (2003) Electronic interactions in metallated polythiophenes: What can be learned from model complexes. *Coord Chem Rev* 246:89–101.
27. Albano VG, *et al.* (2007) Electropolymerized Pd-containing thiophene polymer: A reusable supported catalyst for cross-coupling reactions. *Organometallics* 26:4373–4375.
28. Parr RG, Yang W (1989) *Density-Functional Theory of Atoms and Molecules* (Oxford Univ Press/Clarendon, New York), pp ix, 333.
29. Hohenberg P, Kohn W (1964) Inhomogeneous electron gas. *Phys Rev B* 136:864–871.
30. Kohn W, Sham LJ (1965) Quantum density oscillations in an inhomogeneous electron gas. *Phys Rev* 137:A1697–A1705.
31. Salahub DR, Zerner MC, eds (1989) *The Challenge of d and f Electrons: Theory and Computation; Proceedings of the 3rd Chemical Congress of North America*, ACS Symposium Series (Am Chem Soc, Washington, DC), No 394, p 405.
32. Frisch MJ, *et al.* (2004) Gaussian 03 (Gaussian, Inc, Wallingford, CT), Revision C.02.
33. Wilson JS, *et al.* (2001) The energy gap law for triplet states in Pt-containing conjugated polymers and monomers. *J Am Chem Soc* 123:9412–9417.
34. Burdzinski GT, Ramnauth R, Chisholm MH, Gustafson TL (2006) Direct observation of a ^{1}MLCT state by ultrafast transient absorption spectroscopy in $Mo_2(O_2C\text{-}9\text{-anthracene})_4$. *J Am Chem Soc* 128:6776–6777.
35. Danilov EO, *et al.* (2005) Ultrafast energy migration in platinum(II) diimine complexes bearing pyrenylacetylide chromophores. *J Phys Chem A* 109:2465–2471.
36. Iwamura M, Takeuchi S, Tahara T (2007) Real-time observation of the photoinduced structural change of bis(2,9-dimethyl-1,10-phenanthroline)copper(I) by femtosecond fluorescence spectroscopy: A realistic potential curve of the Jahn-Teller distortion. *J Am Chem Soc* 129:5248–5256.
37. Bhasikuttan AC, Suzuki M, Nakashima S, Okada T (2002) Ultrafast fluorescence detection in tris(2,2′-bipyridine)ruthenium(II) complex in solution: Relaxation dynamics involving higher excited states. *J Am Chem Soc* 124:8398–8405.
38. de Melo JS, Silva LM, Arnaut LG, Becker RS (1999) Singlet and triplet energies of α-oligothiophenes: A spectroscopic, theoretical, and photoacoustic study: Extrapolation to polythiophene. *J Chem Phys* 111:5427–5433.
39. Chen LP, Zhu LY, Shuai ZG (2006) Singlet-triplet splittings and their relevance to the spin-dependent exciton formation in light-emitting polymers: An EOM/CCSD study. *J Phys Chem A* 110:13349–13354.
40. Wong WY, *et al.* (2007) Tuning the absorption, charge transport properties, and solar cell efficiency with the number of thienyl rings in platinum-containing poly(aryleneethynylene)s. *J Am Chem Soc* 129:14372.
41. Byrnes MJ, *et al.* (2005) Observation of ^{1}MLCT and ^{3}MLCT excited states in quadruply bonded Mo_2 and W_2 complexes. *J Am Chem Soc* 127:17343–17352.
42. Chisholm MH, *et al.* (2008) Preparations and photophysical properties of fused and nonfused thienyl bridged MM (M = Mo or W) quadruply bonded complexes. *Inorg Chem* 47:3415–3425.
43. Chen C-Y, *et al.* (2004) Spectroscopy and femtosecond dynamics of type-II CdSe/ZnTe core-shell semiconductor synthesized via the CdO precursor. *J Phys Chem B* 108:10687–10691.
44. Chisholm MH, Macintosh AM (1999) On the mechanism of carboxylate ligand scrambling at Mo_2^{4+} centers: Evidence for a catalyzed mechanism. *Dalton Trans*, 1205–1207.